

Complex fragment emission in low energy light-ion reactions

S. Kundu,* C. Bhattacharya, K. Banerjee, T. K. Rana, S. Bhattacharya, A. Dey, T. K. Ghosh, G. Mukherjee, J. K. Meena, P. Mali,[†] S. Mukhopadhyay, D. Pandit, H. Pai, S. R. Banerjee, and D. Gupta[‡]
Variable Energy Cyclotron Centre, 1/AF, Bidhan Nagar, Kolkata - 700064, INDIA

P. Banerjee
Presidency University, Kolkata - 700073, INDIA

Suresh Kumar, A. Shrivastava, A. Chatterjee, K. Ramachandran, K. Mahata, S. K. Pandit, and S. Santra
Nuclear Physics Division, Bhabha Atomic Research Centre, Mumbai - 400085, INDIA

Inclusive energy spectra of the complex fragments ($3 \leq Z \leq 5$) emitted in the reactions ^{12}C (77 MeV) + ^{28}Si , ^{11}B (64 MeV) + ^{28}Si and ^{12}C (73 MeV) + ^{27}Al (all having the same excitation energy of ~ 67 MeV), have been measured in the angular range of $10^\circ \lesssim \theta_{lab} \lesssim 60^\circ$. The fully energy damped (fusion-fission) and the partially energy damped (deep inelastic) components of the fragment energy spectra have been extracted. It has been found that the yields of the fully energy damped fragments for all the above reactions are in conformity with the respective statistical model predictions. The time scales of various deep inelastic fragment emissions have been extracted from the angular distribution data. The angular momentum dissipation in deep inelastic collisions has been estimated from the data and it has been found to be close to the corresponding sticking limit value.

PACS numbers: 25.70.Jj, 24.60.Dr, 25.70.Lm

I. INTRODUCTION

The phenomenon of complex fragment emission in low- and intermediate-energy nucleus-nucleus collisions has been a subject of intense theoretical [1–8] and experimental [9–43] studies for the last few decades. It is nowadays known from these studies that the origin of the complex fragments may be broadly classified into two major categories, i.e., fusion-fission (FF) and non-fusion (deep inelastic, quasi elastic, breakup, etc.) processes. A large part of the above studies have been devoted to understand the mechanism of complex fragment emission in fusion-fission process for both heavy (typically, $A_{\text{projectile}} + A_{\text{target}} \gtrsim 60$) as well as light compound systems [1–5, 9–16, 20–43]. On the other hand, the properties of deep inelastic (DI) reactions have been studied in details mostly for heavier systems in the past decades (see, for example, [17–19] and references therein) to extract important information about the origins of nuclear relaxation processes, and the data on DI reactions for lighter systems are rather scarce [25, 28–30]. This might be due to the fact that, unlike in the case of heavy systems, the distinction between the DI and the FF processes is rather difficult for light systems, as in the later case there is strong overlap in the elemental distributions of the fragments originating from the two processes. The scenario

becomes further complicated particularly for the reactions involving α -cluster nuclei, where nuclear structure is also known to play an important role in the equilibrium emission of complex fragments. In these cases, in addition to the standard fusion-fission route of fragment emission, the projectile and the target have a finite probability to form a long-lived dinuclear composite, which directly undergoes scission (without the formation of the fully equilibrated compound nucleus) to emit complex fragments. This process, termed as nuclear orbiting [42], has been shown to contribute significantly to the fragment yield in many reactions involving light α -cluster nuclei (e.g., $^{16}\text{O} + ^{12}\text{C}$ [23], $^{20}\text{Ne} + ^{12}\text{C}$ [24, 27, 38, 39], $^{24}\text{Mg} + ^{12}\text{C}$ [43], $^{28}\text{Si} + ^{12}\text{C}$ [40, 41] etc.).

In recent years, a few studies have been made on the α -cluster system $^{40}\text{Ca}^*$ and the neighboring non- α -cluster systems to look into the relationship between equilibrium emission of fragment (and *vis-à-vis* orbiting) and α -clustering. From the study of fragment emission ($6 \leq Z \leq 8$) in the inverse kinematical reaction $^{28}\text{Si} + ^{12}\text{C}$ at energies $29.5 \text{ MeV} < E_{c.m} < 50 \text{ MeV}$ [41], it has been conjectured that orbiting played a crucial role in fully energy-damped fragment emission. Even for the non- α -cluster system with $A_{CN} \simeq 42$ ($^{28}\text{Si} + ^{14}\text{N}$), where the number of open reaction channels was large compared to that of $^{28}\text{Si} + ^{12}\text{C}$ [44], the yields of fully energy-damped fragments ($6 \leq Z \leq 8$) were found to have contributions, though smaller in magnitude, from the orbiting process [45–47].

It will, therefore, be worthwhile to study the emission of lighter fragments ($Z < 6$) in particular, for systems around $A_{CN} \simeq 40$, to extract the contributions of different emission mechanisms, which will be partly complementary to the earlier measurements [41]. Here, we

* skundu@vecc.gov.in, samir.kundu@gmail.com

[†] Present address: Dept. of Physics, University of North Bengal, Silliguri - 734013, INDIA

[‡] Present address: Dept. of Physics and Centre for Astroparticle Physics and Space Science, Bose Institute, Bidhan Nagar, Kolkata - 700091, INDIA

report our study of light fragment ($3 \leq Z \leq 5$) emission from α -cluster system ($^{40}\text{Ca}^*$) produced in ^{12}C (77 MeV) + ^{28}Si reaction, as well as those from the neighboring composite system $^{39}\text{K}^*$ produced at the same excitation energy (~ 67 MeV) via two different reaction channels (^{11}B (64 MeV) + ^{28}Si and ^{12}C (73 MeV) + ^{27}Al); the last two reactions have been chosen to crosscheck the equilibrium decay nature (absence of entrance channel dependence) of the energy damped binary fragment yield in the decay of $^{39}\text{K}^*$. The time scales and the angular momentum dissipation factors for DI fragment emission in these reactions have also been studied.

The article has been arranged as follows. The experimental arrangement has been described in Sec. II. The experimental results and analysis have been presented in Sec. III and the discussions of the results have been given in Sec. IV. Finally, the summary has been given in Sec. V.

II. EXPERIMENT

The experiment has been performed using ^{12}C and ^{11}B ion beams from the BARC - TIFR 14UD Pelletron accelerator at Mumbai. The ^{12}C ion beam of energy 77 MeV was bombarded on a self supporting ^{28}Si target of thickness $\sim 1 \text{ mg/cm}^2$, to produce $^{40}\text{Ca}^*$ at ~ 67 MeV of excitation energy. In addition, the ^{12}C ion beam of energy 73 MeV and the ^{11}B ion beam of energy 64 MeV were bombarded on ^{27}Al (self supporting, $\sim 500 \mu\text{g/cm}^2$), ^{28}Si (thickness same as above) targets, respectively, to produce the same composite $^{39}\text{K}^*$, at the same excitation energy (~ 67 MeV). The fragments ($3 \leq Z \leq 5$) have been detected using Silicon detector (surface barrier) telescopes ($\sim 10\mu\text{m } \Delta E$, $\sim 350\mu\text{m } E$). The calibration of the telescopes were done using the elastically scattered ^{12}C , ^{11}B ions from Al, Si and Au targets. The inclusive energy distributions of the emitted fragments for each reaction have been measured in the laboratory angular range of $\sim 12^\circ$ to 55° [$\sim 18^\circ$ - 82° in the center-of-mass (c.m.) frame]. The total systematic error in the data, arising from the uncertainties in the measurements of the solid angle, the target thickness, and the calibration of current digitizer have been estimated to be $\approx 12\%$.

III. ENERGY SPECTRA

Typical energy spectra of the fragments ($3 \leq Z \leq 5$) emitted in ^{11}B (64 MeV) + ^{28}Si , ^{12}C (73 MeV) + ^{27}Al and ^{12}C (77 MeV) + ^{28}Si reactions have been shown in Fig. 1. It is clear from the figure that the shapes of the fragment energy spectra obtained in the three reactions are quite different. This is mainly due to the variation of the relative contributions of DI and FF processes in each case.

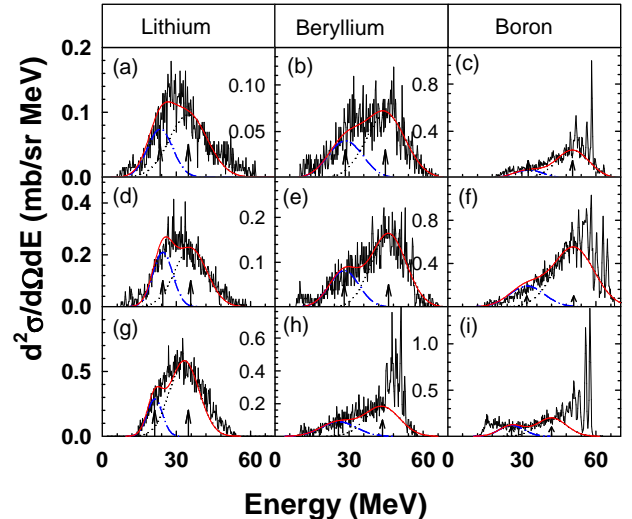


FIG. 1. (Color online) Typical energy spectra of the fragments measured for the reactions $^{12}\text{C} + ^{28}\text{Si}$ (a) – (c), $^{12}\text{C} + ^{27}\text{Al}$ (d) – (f) and $^{11}\text{B} + ^{28}\text{Si}$ (g) – (i) at $\theta_{lab} = 17.5$ (a) – (h) and 30° (i). The blue dash-dotted, the black dotted, and the red solid curves represent the contributions of the FF, the DI, and the sum (FF + DI), respectively. The left and the right arrows correspond to the centroids of FF and DI components of energy distributions, respectively.

In order to extract the FF and the DI components, the energy distribution of each fragment at each angle has been fitted with two Gaussian functions in two steps, as prescribed in [29, 30]. In the first step, the FF contribution has been obtained by fitting the energy distribution with a Gaussian having the centroid energy obtained from Viola systematics, duly corrected for the asymmetric factor [48, 49]. The width of the Gaussian has been obtained by fitting the lower energy tail of the spectrum. The FF component of the energy spectrum thus obtained has then been subtracted from the full energy spectrum. In the next step, the DI component has been obtained by fitting the subtracted energy spectrum with a second Gaussian. The contributions of FF and DI components thus obtained (for each fragment) have been displayed in Fig. 1. In each spectrum, the arrow at lower (higher) energy indicates the position of the centroid of the FF (DI) energy distribution.

A. Study of FF fragments

1. Angular distribution

The FF fragment angular distribution has been obtained by integrating the corresponding Gaussian extracted from the energy distribution. The c.m. angular distributions ($d\sigma/d\Omega_{FF}$) of the FF fragments (Li, Be and B) have been shown in Fig. 2. It is evident from the figure that the angular distributions of all FF fragments

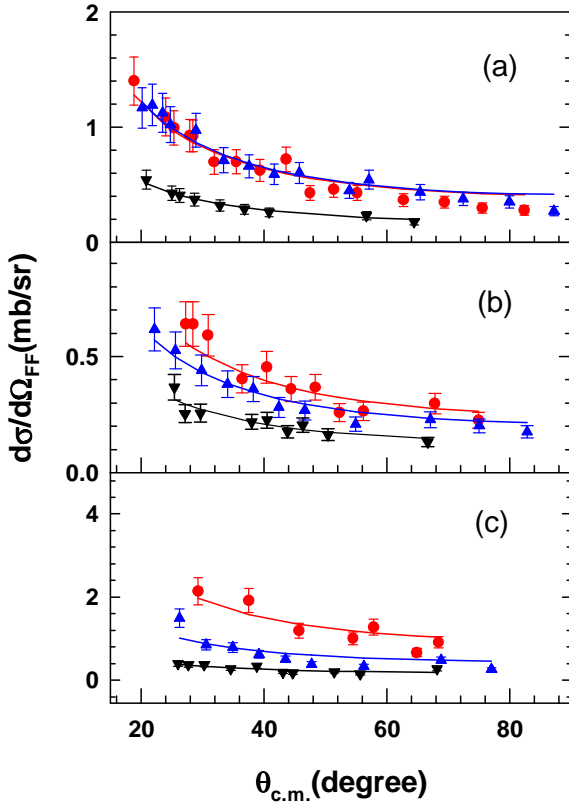


FIG. 2. (Color online) The c.m. angular distributions of the fragments Li (a), Be (b) and B (c). Solid circles (red), triangles (blue) and inverted triangles (black) correspond to the experimental data for the reactions $^{11}\text{B} + ^{28}\text{Si}$, $^{12}\text{C} + ^{27}\text{Al}$ and $^{12}\text{C} + ^{28}\text{Si}$, respectively. Solid curves are fit to the data with the function $f(\theta_{c.m.}) \propto 1/\sin\theta_{c.m.}$.

follow $\sim 1/\sin\theta_{c.m.}$ dependence, which is characteristic of the fission-like decay of an equilibrated composite system. It is also clear from the figure that the yields of Li and Be are almost same at all angles for $^{11}\text{B} + ^{28}\text{Si}$ and $^{12}\text{C} + ^{27}\text{Al}$ reactions. It has further been observed that yield of the fragment B in $^{11}\text{B} + ^{28}\text{Si}$ reaction was more than that in $^{12}\text{C} + ^{27}\text{Al}$ reaction. It has also been observed that the fragment angular yields for the reactions $^{11}\text{B} + ^{28}\text{Si}$ and $^{12}\text{C} + ^{27}\text{Al}$ are a little higher (though nearly comparable in magnitude) than those obtained in $^{12}\text{C} + ^{28}\text{Si}$ reaction at the same excitation energy.

2. Total fragment yield

The experimental angle integrated yields of the FF fragments for all the three reactions have been shown in Fig. 3. It is found that the yields of Li and Be in $^{11}\text{B} + ^{28}\text{Si}$ and $^{12}\text{C} + ^{27}\text{Al}$ reactions are nearly the same; the absence of any entrance channel dependence confirms their compound nuclear origin. It has also been observed that the yields of these fragments are comparable to those obtained in $^{12}\text{C} + ^{28}\text{Si}$ reaction. The yield of B in the re-

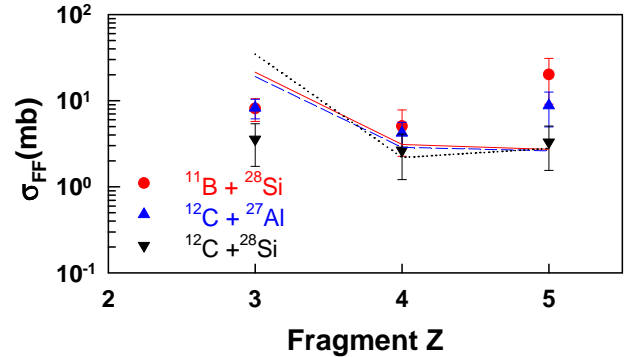


FIG. 3. (Color online) The total FF fragment cross sections for the three reactions. The solid circles (red), triangles (blue), and inverted triangles (black) correspond to the experimental data for $^{11}\text{B} + ^{28}\text{Si}$, $^{12}\text{C} + ^{27}\text{Al}$, and $^{12}\text{C} + ^{28}\text{Si}$ reactions, respectively. The solid (red), dashed (blue) and dotted (black) lines are the corresponding theoretical predictions.

action $^{11}\text{B} + ^{28}\text{Si}$ has been found to be slightly more than that obtained in the other two reactions, which might be due to the contamination from the beam-like channels in the former case, where B was the projectile.

The experimental FF fragment yields have been compared with the theoretical estimates of the same obtained from the extended Hauser-Feshbach model (EHFM) [50]. The values of the critical angular momenta have been obtained from the experimental fusion cross section data, wherever available [51, 52]; otherwise, they have been obtained from the dynamical trajectory model calculations with realistic nucleus-nucleus interaction and the dissipative forces generated self-consistently through stochastic nucleon exchanges [53]. The values of the critical angular momentum, l_{cr} , for all the three systems, have been the same ($27\hbar$). The calculated fragment emission cross sections have been shown in Fig. 3. It is seen from the figure that in all three cases, the theoretical predictions are nearly the same and are in fair agreement with the experimental results.

B. Study of DI fragments

1. Angular distribution

The DI component of the fragment angular distribution has been obtained by integrating the respective Gaussian extracted from the energy distribution data. The c.m. angular distributions of the DI components $d\sigma/d\Omega_{DI}$ of the fragments have been displayed in Fig. 4. It is found that they fall much faster than $\sim 1/\sin\theta_{c.m.}$ distribution, indicating shorter lifetime of the composite system. Such lifetimes are incompatible with the formation of an equilibrated compound nucleus, but may still reflect significant energy damping within the deep-inelastic collision mechanism. It is possible to estimate the lifetime of the intermediate di-nuclear complex using

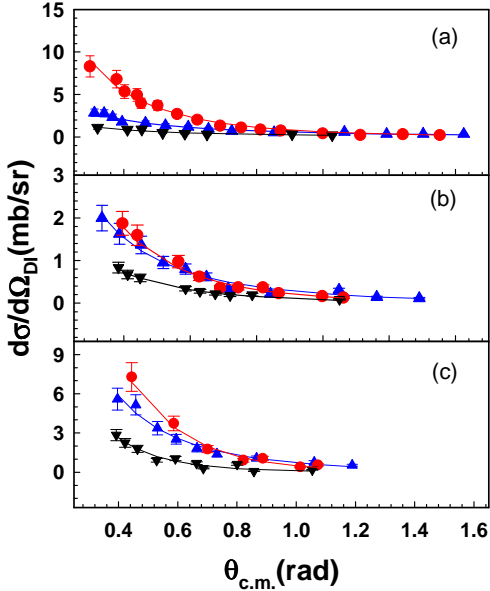


FIG. 4. (Color online) The c.m. angular distributions of the DI fragments [Li (a), Be (b), and, B (c)]. The solid circles (red), triangles (blue), and inverted triangles (black) correspond to the experimental data for $^{11}\text{B} + ^{28}\text{Si}$, $^{12}\text{C} + ^{27}\text{Al}$, and $^{12}\text{C} + ^{28}\text{Si}$ reactions, respectively; the solid lines are the fits to the data (see text).

a diffractive Regge-pole model [32, 54] from these measured forward peaked angular distributions. The angular distributions have been fitted using the following expression,

$$(d\sigma/d\Omega)_{DI} = (C/\sin\theta_{c.m.})(e^{-\theta_{c.m.}/\omega\tau_{DI}}). \quad (1)$$

The expression describes the decay of a di-nucleus rotating with an angular velocity $\omega = \hbar l/\mu R^2$, where μ is the reduced mass of the system, l is the angular momentum ($l_{cr} < l < l_{gr}$; l_{gr} , l_{cr} being the grazing and the critical angular momenta, respectively), R represents the distance between the two centres of the di-nucleus and τ_{DI} is the time interval during which the two nuclei remain in a solid contact in the form of the rotating di-nucleus. The value of the ‘life angle’ $\alpha (= \omega\tau_{DI})$ decides the time scale of the reaction. The forward peaked angular distributions (and small values of α) are associated with the fast processes; on the contrary, large values of α ($\gtrsim 2\pi$, associated with longer times as compared to the di-nucleus rotation period $\tau_{eq} = 2\pi/\omega$), correspond to the long lived configurations and lead to isotropic angular distributions. The time scales for different DI fragments (Li, Be and B) thus obtained have been shown in Fig. 5 for comparison. It is seen that, in all reactions, the time scale decreases as the fragment charge increases, which is in conformity with a previous study by Mikumo *et al.* [54]. This is expected because the heavier fragments (nearer to the projectile) require less nucleon exchange and therefore less time; on the other hand, the

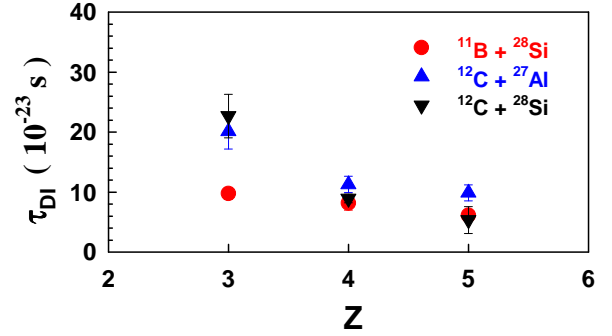


FIG. 5. (Color online) The emission time scales of different DI fragments.

emission of lighter fragments requires more nucleon exchange and therefore longer times. The emission time scales of the fragments are related to the number of nucleons exchanged on the average. This explains why the emission time scales of $^{12}\text{C} + ^{27}\text{Al}$ and $^{12}\text{C} + ^{28}\text{Si}$ reactions are nearly the same for all fragments. On the other hand, in the case of $^{11}\text{B} + ^{28}\text{Si}$ reaction, net nucleon exchange is one less to reach any particular fragment; so the corresponding time scales are less. For example, in terms of net nucleon exchange, the emission time scale of Li (Be) from $^{11}\text{B} + ^{28}\text{Si}$ should be comparable to that of Be (B) from $^{12}\text{C} + ^{27}\text{Al}$ and $^{12}\text{C} + ^{28}\text{Si}$ reactions, which is actually the case (Fig. 5).

2. Average Q value

The average Q values ($\langle Q_{DI} \rangle$) of the DI fragments, estimated from the fragment kinetic energies assuming two-body kinematics, have been displayed in Fig. 6 as a function of the c.m. angle. It is found that, for all fragments, the $\langle Q_{DI} \rangle$ values tend to decrease with the increase of angles for $\theta_{c.m.} \lesssim 40^\circ$, and then gradually become nearly constant. It implies that, beyond this point, the kinetic energy damping is complete and dynamic equilibrium has been established before the scission of the di-nuclear composite takes place.

3. Total fragment yield

The experimental angle integrated yields of the DI fragments for $^{11}\text{B} + ^{28}\text{Si}$, $^{12}\text{C} + ^{27}\text{Al}$, and, $^{12}\text{C} + ^{28}\text{Si}$ reactions are shown in Fig. 7. It is found that the DI yields of all the fragments emitted in B+Si reaction are slightly higher than those obtained in C+Al and C+Si reactions. This may be due to the variation of the probability of net nucleon exchange. In addition, the DI fragment yield in C+Si reaction tends to be lower than that for C+Al reaction.

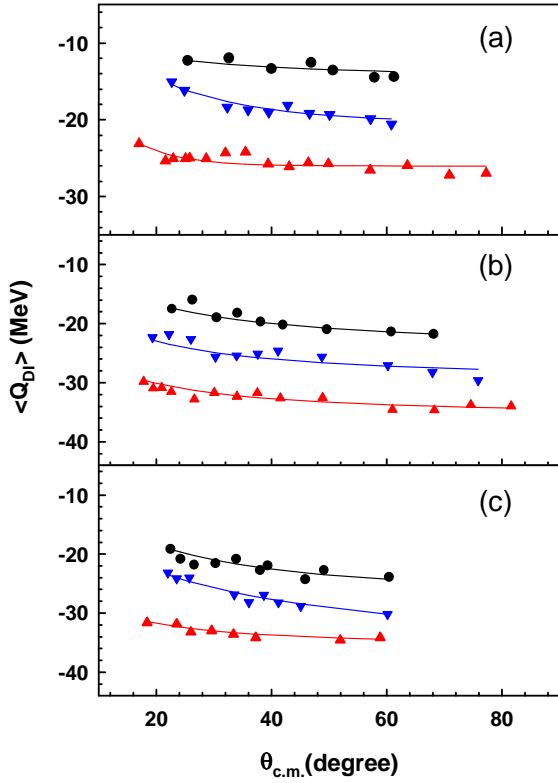


FIG. 6. (Color online) The average Q values, $\langle Q_{DI} \rangle$, plotted as function of $\theta_{c.m.}$ for Li (red triangle), Be (blue inverted triangle), and B (black solid circle) emitted in (a) $^{11}\text{B} + ^{28}\text{Si}$, (b) $^{12}\text{C} + ^{27}\text{Al}$, and (c) $^{12}\text{C} + ^{28}\text{Si}$ reactions. Solid lines are plotted to guide the eye.

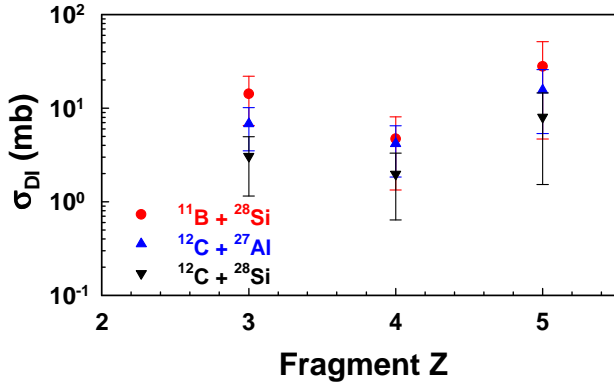


FIG. 7. (Color online) Total DI cross sections of the fragments obtained in three different reactions.

IV. DISCUSSIONS

A. FF fragment emission

In the case of the decay of $^{40}\text{Ca}^*$, the measured FF fragment yields ($3 \leq Z \leq 5$) have been found to be in good agreement with the respective statistical model predictions (see Fig. 3), indicative of the compound nuclear

origin of these fragments. However, a previous study on the binary decay of the same system [40] (using inverse kinematical reaction) had reported an enhancement of fragment ($6 \leq Z \leq 8$) yield over the statistical model prediction and thereby conjectured the presence of orbiting mechanism. In the case of the decay of $^{39}\text{K}^*$, the absence of any entrance channel dependence (between B+Si and C+Al systems) and the matching of the extracted FF fragment yields with the respective EHFm predictions (see Fig. 3) have been clearly suggestive of the compound nuclear origin of these fragments.

B. Angular momentum dissipation factor

The angular momentum dissipation in DI collision is important to understand the variation of the mean kinetic energies of the fragments as well as the energy damping mechanism in general. For heavy systems, the angular momentum dissipation is experimentally estimated using the α -particle angular distribution and the γ -ray multiplicity data and it is known that the rigid rotation limit is usually reached in these systems [19]. For the light systems, the angular momentum transfer is generally estimated from the total kinetic energy of the rotating di-nuclear system, E_k , which is given by,

$$E_k = V_N(d) + f^2 \frac{\hbar^2 l_i(l_i + 1)}{2\mu d^2}, \quad (2)$$

where $V_N(d)$ is the contribution from Coulomb and nuclear forces at di-nuclear separation distance d , μ is the reduced mass of the di-nuclear configuration, l_i is the relative angular momentum in the entrance channel and f is the numerical factor denoting the fraction of the angular momentum transferred. For these light systems, there have been indications of large dissipation of relative angular momentum [39], which might be partly due to the ambiguity in the determination of the magnitude of angular momentum dissipation, as both d and f are unknown quantities (see Ref. [30] and references therein). A simple prescription for estimating both f and d was described in Ref. [30], where it has been shown that the fraction of angular momentum transfer for fully energy-damped DI collision of a few light systems is close to the corresponding rigid rotation limit (sticking limit). To see whether this trend is valid in general for DI collisions of light systems, angular momentum dissipation factor, f , for each exit channel mass asymmetry has been extracted for all the reactions, which have been displayed in Fig. 8. For the present calculations, the separation distance d between the two fragments has been estimated from the scission point configuration corresponding to the respective asymmetric mass splitting [49], and the value of initial angular momentum l_i has been taken to be equal to the critical angular momentum for fusion, l_{cr} .

It is observed from Fig. 8 that for all the three reactions considered, the experimental values of the

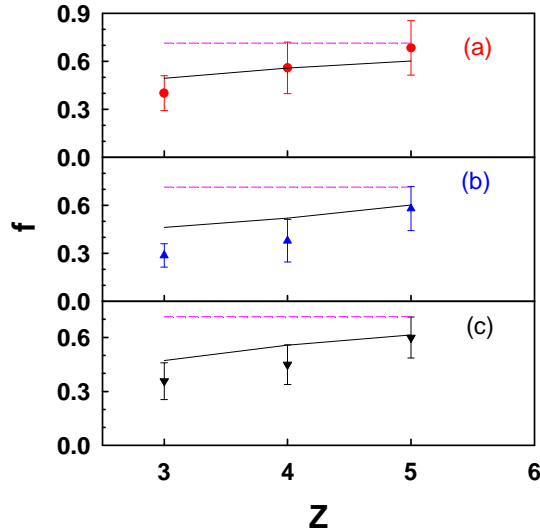


FIG. 8. (Color online) The variation of angular momentum dissipation factor f with fragment. The solid circles (red), solid triangles (blue), and inverted triangles (black) are the extracted values of f for (a) $^{11}\text{B} + ^{28}\text{Si}$, (b) $^{12}\text{C} + ^{27}\text{Al}$, and (c) $^{12}\text{C} + ^{28}\text{Si}$ reactions, respectively. The solid (black) and dotted (pink) curves correspond to the sticking limit and the rolling limit predictions for the same, respectively.

mean angular momentum dissipation are more than those predicted under the rolling condition; however, the corresponding sticking limit predictions of f are in fair agreement with the experimental values of the same within the error bar. In all cases, the discrepancy is more for the lighter fragments, and it gradually decreases for the heavier fragments. This may be explained in terms of the following qualitative argument. Microscopically, friction is generated due to stochastic exchange of nucleons between the reacting partners through the window formed by the overlap of the density distributions of the two. Stronger friction essentially means larger degree of density overlap and more nucleon exchange. The lighter DI fragment (corresponds to more net nucleon transfer) originates from deeper collision, for which the interaction time is also larger as seen in Fig. 5. Therefore, the angular momentum dissipation, originating due to the stochastic nucleon exchange, should also be more, which, at least qualitatively, explains the observed trend.

V. CONCLUSION

Light fragment ($3 \leq Z \leq 5$) emission in ^{11}B (64 MeV) + ^{28}Si , ^{12}C (73 MeV) + ^{27}Al and ^{12}C (77 MeV) + ^{28}Si reactions have been studied in details. The inclusive double differential cross sections for the fragments emitted in these reactions have been measured in the angular range of $\sim 12^\circ$ to 55° . The energy distributions of the frag-

ments have been fitted with two Gaussians to extract the fusion-fission and the deep-inelastic components. The c.m. angular distributions of the fusion-fission fragments have been found to follow $1/\sin\theta_{c.m.}$ dependence, which signifies the emission of these fragments from a long-lived equilibrated composite. The total elemental cross-sections of the FF fragments have been obtained by integrating the angular distributions of the FF components. In the case of $^{12}\text{C} + ^{28}\text{Si}$ reaction, the integrated yields of the light fragments ($3 \leq Z \leq 5$) have been found to be in fair agreement with the statistical model predictions. It is interesting to note here that a previous study on fragment decay from the same system ($^{40}\text{Ca}^*$, produced through inverse kinematical reaction $^{28}\text{Si} + ^{12}\text{C}$ at same excitation energy [40]) has shown signatures of enhancement in fragment yield (for relatively heavier fragments; $6 \leq Z \leq 8$) over those predicted by the statistical model.

We have also studied fragment emission from the nearest non- α cluster system, $^{39}\text{K}^*$, produced at the same excitation energy (67 MeV) via two different entrance channels viz. ^{11}B (64 MeV) + ^{28}Si and ^{12}C (73 MeV) + ^{27}Al respectively. It has been found that the angular distributions of the FF fragments ($3 \leq Z \leq 5$) obtained in these reactions are almost similar and follow the $1/\sin\theta_{c.m.}$ dependence, indicating the emission from an equilibrated source. The absence of any entrance channel dependence is consistent with the compound nuclear origin of these fragments.

The DI component of the fragment ($3 \leq Z \leq 5$) energy distribution in all the three reactions has been studied in details. It has been shown that the DI fragment angular distribution falls much faster than $1/\sin\theta_{c.m.}$ distribution. The time scale of the DI process has been estimated from these DI angular distributions. It has been observed that for all these reactions, the time scale, which is related to net nucleon transfer, decreases as the fragment charge increases (closer to the projectile charge). It has also been observed that the average Q values for the DI fragments decrease with the increase of emission angle and saturate at higher angles, signifying a saturation in energy damping process beyond these angles. Assuming a compact exit channel configuration (estimated from the extracted FF part of the spectra), the angular momentum dissipation factor, f , for the DI process has been extracted. For all the three reactions, the experimental values of f have been found to be in fair agreement with the corresponding sticking limit predictions.

ACKNOWLEDGMENTS

The authors thank the staff of the Bhabha Atomic Research Centre, Tata Institute of Fundamental Research (BARC - TIFR) Pelletron accelerator, Mumbai, for smooth running of the machine.

-
- [1] L. G. Moretto, Nucl. Phys. A **247**, 211 (1975).
- [2] L. G. Moretto and G. J. Wozniak, Prog. Part. Nucl. Phys. **21**, 401 (1988), and references therein.
- [3] R. J. Charity, D. R. Bowman, Z. H. Liu, R. J. McDonald, M. A. McMahan, G. J. Wozniak, L. G. Moretto, S. Bradley, W. L. Kehoe, and A. C. Mignerey, Nucl. Phys. A **476**, 516 (1988).
- [4] R. J. Charity, M. A. McMahan, G. J. Wozniak, R. J. McDonald, L. G. Moretto, D. G. Sarantites, L. G. Sobotka, G. Guarino, A. Pantaleo, L. Fiore, A. Gobbi, and K. D. Hildenbrand, Nucl. Phys. A **483**, 371 (1988).
- [5] S. A. Kalandarov, G. G. Adamian, N. V. Antonenko, W. Scheid, and J. P. Wileczko, Phys. Rev. C **84**, 064601 (2011).
- [6] S. J. Sanders, Phys. Rev. C **44**, 2676 (1991).
- [7] A. K. Dhara, C. Bhattacharya, S. Bhattacharya, and K. Krishan, Phys. Rev. C **48**, 1910 (1993).
- [8] A. Szanto de Toledo, S. J. Sanders, and C. Beck, Phys. Rev. C **56**, 558 (1997).
- [9] L. G. Sobotka, M. L. Padgett, G. J. Wozniak, G. Guarino, A. J. Pacheco, L. G. Moretto, Y. Chan, R. G. Stokstad, I. Tserruya, and S. Wald, Phys. Rev. Lett. **51**, 2187 (1983).
- [10] L. G. Sobotka, M. A. McMahan, R. J. McDonald, C. Signarbieux, G. J. Wozniak, M. L. Padgett, J. H. Gu, Z. H. Liu, Z. Q. Yao, and L. G. Moretto, Phys. Rev. Lett. **53**, 2004 (1984).
- [11] M. A. McMahan, L. G. Moretto, M. L. Padgett, G. J. Wozniak, L. G. Sobotka, and M. G. Mustafa, Phys. Rev. Lett. **54**, 1995 (1985).
- [12] T. Kozik, J. Buschmann, K. Grotowski, H. J. Gils, N. Heide, J. Kiener, H. Klewe-Nebenius, H. Rebel, S. Zagromski, A. J. Cole, and S. Micek, Z. Phys. A **326**, 421 (1987).
- [13] K. Grotowski, Z. Majka, R. Planeta, M. Szczodrak, Y. Chan, G. Guarino, L. G. Moretto, D. J. Morrissey, L. G. Sobotka, R. G. Stokstad, I. Tserruya, S. Wald, and G. J. Wozniak, Phys. Rev. C **30**, 1214 (1984).
- [14] K. Grotowski, J. Ilnicki, T. Kozik, J. Lukasik, S. Micek, Z. Sosin, A. Wieloch, N. Heide, H. Jelitto, I. Kiener, H. Rebel, S. Zagromski, and A. J. Cole, Phys. Lett. B **223**, 287 (1989).
- [15] K. Kwiatkowski, J. Bashkin, H. Karwowski, M. Fatyga, and V. E. Viola, Phys. Lett. B **171**, 41 (1986).
- [16] G. Ademard, J. P. Wileczko, J. Gomez del Campo, M. La Commara, E. Bonnet, M. Vigilante, A. Chbihi, J. D. Frankland, E. Rosato, G. Spadaccini, S. A. Kalandarov, C. Beck, S. Barlini, B. Borderie, R. Bougault, R. Dayras, G. De Angelis, J. De Sanctis, V. L. Kravchuk, P. Lautesse, N. Le Neindre, J. Moisan, A. D'Onofrio, M. Parlog, D. Pierroutsakou, M. F. Rivet, M. Romoli, R. Roy, G. G. Adamian, and N. V. Antonenko, Phys. Rev. C **83**, 054619 (2011).
- [17] W. U. Schröder and J. R. Huizenga, Ann. Rev. Nucl. Sci. **27**, 465 (1977).
- [18] W. U. Schröder and J. R. Huizenga, *Treatise on Heavy-Ion Science*, edited by D. A. Brombley, Vol. 2 (Plenum Press, New York and London, 1984) p. 113.
- [19] L. G. Sobotka, C. C. Hsu, G. J. Wozniak, G. U. Rattazzi, R. J. McDonald, A. J. Pacheco, and L. G. Moretto, Phys. Rev. Lett. **46**, 887 (1981).
- [20] S. Cavallaro, E. De Filippo, G. Lanzanò, A. Pagano, M. L. Sperduto, R. Dayras, R. Legrain, E. Pollicchio, C. Beck, B. Djerroud, R. M. Freeman, F. Haas, A. Hachem, B. Heusch, D. Mahboub, A. Morsad, R. Nouicer, and S. J. Sanders, Phys. Rev. C **57**, 731 (1998).
- [21] N. Carlin Filho, M. M. Coimbra, N. Added, R. M. dos Anjos, L. Fante, M. C. S. Figueira, V. Guimaraes, E. M. Szanto, A. Szanto de Toledo, and O. Civitarese, Phys. Rev. C **40**, 91 (1989).
- [22] S. J. Sanders, A. Szanto de Toledo, and C. Beck, Phys. Rep. **311**, 487 (1999), and references therein.
- [23] S. Kundu, A. Dey, K. Banerjee, T. K. Rana, S. Mukhopadhyay, D. Gupta, R. Saha, S. Bhattacharya, and C. Bhattacharya, Phys. Rev. C **78**, 044601 (2008).
- [24] A. Dey, C. Bhattacharya, S. Bhattacharya, S. Kundu, K. Banerjee, S. Mukhopadhyay, D. Gupta, T. Bhattacharjee, S. R. Banerjee, S. Bhattacharyya, T. K. Rana, S. K. Basu, R. Saha, K. Krishan, A. Mukherjee, D. Bandopadhyay, and C. Beck, Phys. Rev. C **76**, 034608 (2007), and references therein.
- [25] A. Dey, C. Bhattacharya, S. Bhattacharya, T. K. Rana, S. Kundu, K. Banerjee, S. Mukhopadhyay, S. R. Banerjee, D. Gupta, and R. Saha, Phys. Rev. C **75**, 064606 (2007), and references therein.
- [26] S. Szilner, F. Haas, Z. Basrak, R. M. Freeman, A. Morsad, and M. P. Nicoli, Nucl. Phys. A **779**, 21 (2006).
- [27] C. Bhattacharya, A. Dey, S. Kundu, K. Banerjee, S. Bhattacharya, S. Mukhopadhyay, D. Gupta, T. Bhattacharjee, S. R. Banerjee, S. Bhattacharyya, T. Rana, S. K. Basu, R. Saha, S. Bhattacharjee, K. Krishan, A. Mukherjee, D. Bandopadhyay, and C. Beck, Phys. Rev. C **72**, 021601 (2005).
- [28] A. Pop, A. Andronic, I. Berceanu, M. Duma, Moisă, M. Petrovici, V. Simion, A. Bonasera, G. Immé, G. Lanzanò, A. Pagano, G. Raciti, N. Colonna, G. d'Erasio, A. Pantaleo, H. Feldmeier, and J. Schnack, Nucl. Phys. A **679**, 793 (2001), and references therein.
- [29] C. Bhattacharya, K. Mullick, S. Bhattacharya, K. Krishan, T. Bhattacharjee, P. Das, S. R. Banerjee, D. N. Basu, A. Ray, S. K. Basu, and M. B. Chatterjee, Phys. Rev. C **66**, 047601 (2002).
- [30] C. Bhattacharya, S. Bhattacharya, T. Bhattacharjee, A. Dey, S. Kundu, S. R. Banerjee, P. Das, S. K. Basu, and K. Krishan, Phys. Rev. C **69**, 024607 (2004), and references therein.
- [31] C. Bhattacharya, D. Bandyopadhyay, S. K. Basu, S. Bhattacharya, K. Krishan, G. S. N. Murthy, A. Chatterjee, S. Kailas, and P. Singh, Phys. Rev. C **54**, 3099 (1996).
- [32] C. Beck, R. Nouicer, D. Mahboub, B. Djerroud, R. M. Freeman, A. Hachem, T. Matsuse, S. Cavallaro, E. De Filippo, G. Lanzanò, A. Pagano, M. L. Sperduto, R. Dayras, E. Berthoumieux, R. Legrain, and E. Pollicchio, Eur. Phys. J. A **2**, 281 (1998).
- [33] C. Beck, D. Mahboub, R. Nouicer, T. Matsuse, B. Djerroud, R. M. Freeman, F. Haas, A. Hachem, A. Morsad, M. Youlal, S. J. Sanders, R. Dayras, J. P. Wileczko, E. Berthoumieux, R. Legrain, E. Pollacco, S. Cavallaro, E. De Filippo, G. Lanzanò, A. Pagano, and M. L. Sperduto, Phys. Rev. C **54**, 227 (1996).

- [34] S. P. Barrow, R. W. Zurmühle, D. R. Benton, Y. Miao, Q. Li, P. H. Kutt, Z. Liu, C. Lee, N. G. Wimer, and J. T. Murgatroyd, Phys. Rev. C **52**, 3088 (1995).
- [35] K. A. Farrar, S. J. Sanders, A. K. Dummer, A. T. Hasan, F. W. Prosser, B. B. Back, I. G. Bearden, R. R. Betts, M. P. Carpenter, B. Crowell, M. Freer, D. J. Henderson, R. V. F. Janssens, T. L. Khoo, T. Lauritsen, Y. Liang, D. Nisius, A. H. Wuosmaa, C. Beck, R. M. Freeman, S. Cavallaro, A. Szanto de Toledo, and et al., Phys. Rev. C **54**, 1249 (1996).
- [36] R. M. Anjos, N. Added, N. Carlin, L. Fante, M. C. S. Figueira, R. Matheus, H. R. Schelin, E. M. Szanto, C. Tenreiro, A. Szanto de Toledo, and S. J. Sanders, Phys. Rev. C **48**, R2154 (1993).
- [37] C. Beck, B. Djerroud, F. Haas, R. M. Freeman, A. Hachem, B. Heusch, A. Morsad, M. Vuillet-A-Cilles, and S. J. Sanders, Phys. Rev. C **47**, 2093 (1993).
- [38] D. Shapira, J. L. C. Ford, J. Gomez del Campo, R. G. Stokstad, and R. M. DeVries, Phys. Rev. Lett. **43**, 1781 (1979).
- [39] D. Shapira, J. L. C. Ford Jr., and J. Gomez del Campo, Phys. Rev. C **26**, 2470 (1982).
- [40] D. Shapira, R. Novotny, Y. C. Chan, K. A. Erb, J. L. C. Ford Jr., J. C. Peng, and J. D. Moses, Phys. Lett. B **114**, 111 (1982).
- [41] D. Shapira, D. Schull, J. L. C. Ford Jr., B. Shivakumar, R. L. Parks, R. A. Cecil, and S. T. Thornton, Phys. Rev. Lett. **53**, 1634 (1984).
- [42] B. Shivakumar, S. Ayik, B. A. Harmon, and D. Shapira, Phys. Rev. C **35**, 1730 (1987).
- [43] W. Dünnweber, A. Glaesner, W. Hering, D. Konnerth, R. Ritzka, W. Trombik, J. Czakański, and W. Zipper, Phys. Rev. Lett. **61**, 927 (1988).
- [44] C. Beck, Y. Abe, N. Aissaoui, B. Djerroud, and F. Haas, Phys. Rev. C **49**, 2618 (1994).
- [45] B. Shivakumar, D. Shapira, P. H. Stelson, M. Beckerman, B. A. Harmon, K. Teh, and D. A. Bromley, Phys. Rev. Lett. **57**, 1211 (1986).
- [46] B. Shivakumar, D. Shapira, P. H. Stelson, S. Ayik, B. A. Harmon, K. Teh, and D. A. Bromley, Phys. Rev. C **37**, 652 (1988).
- [47] S. Ayik, D. Shapira, and B. Shivakumar, Phys. Rev. C **38**, 2610 (1988).
- [48] V. E. Viola, K. Kwiatkowski, and M. Walker, Phys. Rev. C **31**, 1550 (1985).
- [49] C. Beck, B. Djerroud, F. Haas, R. M. Freeman, A. Hachem, B. Heusch, A. Morsad, M. Youlal, Y. Abe, A. Dayras, J. P. Wieleczko, B. T. Matsuse, and S. M. Lee, Z. Phys. A **343**, 309 (1992).
- [50] T. Matsuse, C. Beck, R. Nouicer, and D. Mahboub, Phys. Rev. C **55**, 1380 (1997).
- [51] M. F. Vineyard, J. F. Mateja, C. Beck, S. E. Atencio, L. C. Dennis, A. D. Frawley, D. J. Henderson, R. V. F. Janssens, K. W. Kemper, D. G. Kovar, C. F. Maguire, S. J. Padalino, F. W. Prosser, G. S. F. Stephans, M. A. Tiede, B. D. Wilkins, and R. A. Zingarelli, Phys. Rev. C **47**, 2374 (1993).
- [52] M. Rousseau, C. Beck, C. Bhattacharya, V. Rauch, O. Dorvaux, K. Eddahbi, C. Enaux, R. M. Freeman, F. Haas, D. Mahboub, R. Nouicer, P. Papka, O. Stezowski, S. Szilner, A. Hachem, E. Martin, S. J. Sanders, A. K. Dummer, and A. Szanto de Toledo, Phys. Rev. C **66**, 034612 (2002).
- [53] S. Bhattacharya, K. Krishan, S. K. Samaddar, and J. N. De, Phys. Rev. C **37**, 2916 (1988).
- [54] T. Mikumo, M. Sasagase, M. Sato, T. Ooi, Y. Higashi, Y. Nagashima, and M. Yamanouchi, Phys. Rev. C **21**, 620 (1980).